THz Letters

Loss and Dispersion Limitations in mm-Wave Dielectric Waveguides for High-Speed Links

Nemat Dolatsha, Cheng Chen, and Amin Arbabian

***Abstract*—We investigate the fundamental physical constraints and tradeoffs in common millimeter-wave dielectric waveguides proposed for high speed links. We consider waveguides with different geometries, dimensions and operating frequencies, and show that the capacity of optimized longer links is limited by the dispersion and not necessarily the loss. In our analysis, the required capacity and distance determine the choice of waveguide and the operating frequency, which would then determine the energy efficiency of the link. Our generic theoretical analyses are in agreement with the measurements presented in the recent literature.**

***Index Terms*—Attenuation, dispersion, dielectric waveguide, mm-wave, mm-wave communication.**

I. Introduction

ALONG with the exponential growth of data traffic arising from emerging mobile and web applications, there has been an increasing interest in ultra high speed communication links [1]. In conventional planar aggregated electrical interconnects, high attenuation, dispersion, cross-talk, and impedance mismatch pose limitations on the available bandwidth-per-pitch and result in substantially high power consumption for increasing the data rate over ranges longer than few meters [2]. On the other end of spectrum, optical fiber links with very low attenuation and relatively large bandwidth have been extensively used for long-range communication [3]. However, the associated power and cost overhead due to electro-optical modules and precision packaging limit adaptability for short-range applications [4].

Recently, mm-wave dielectric waveguides with relatively large bandwidth and low attenuation, and being compatible with CMOS integration, have been proposed for short-range high-speed links [5]–[8]. A good energy efficiency of around 2 pJ/bit was reported in [6] and [7]. However, despite the large transmission bandwidth of the waveguides, the maximum capacity achieved for links with few meter lengths is limited to few Gbps. In this paper, we investigate the source of this bandwidth limitation in an analytical framework that includes the fundamental physical constraints (such as attenuation, dispersion) in common mm-wave dielectric waveguides. We discuss the tradeoffs in using different waveguide geometries, dimensions, and operating frequencies for achieving higher capacity at different lengths. We show that higher capacity in such links is primarily limited by dispersion rather than attenuation. Our analysis is an initial step in optimally exploiting the fundamental capacity of dielectric waveguides.

Manuscript received May 02, 2016; accepted May 24, 2016. Date of publication June 29, 2016; date of current version July 08, 2016.

The authors are with the Electrical Engineering Department, Stanford University, Stanford, CA 94305 USA (e-mail: nematd@stanford.edu; cchen91@stanford.edu; arbabian@stanford.edu).

Color versions of one or more of the figures in this letter are available online at http://ieeexplore.ieee.org.

Digital Object Identifier 10.1109/TTHZ.2016.2574326

II. Physical Characteristics of the Channel

As attenuation and dispersion are the fundamental channel characteristics in communication links, we first investigate these parameters for different waveguides.

A. Waveguide Attenuation

In general, the attenuation constant α of a straight waveguide made of a single dielectric material originates from the dielectric loss tangent tan δ [9]

$$\alpha \propto \varepsilon_r R \ \tan\delta/\lambda_0 \ (\mathrm{dB/m}) \tag{1}$$

which indicates that the attenuation is proportional to dielectric constant ε_r, fraction of power propagating inside the waveguide material *R*, loss tangent tan δ, and the operating frequency (inverse of free space wavelength λ_0).

B. Waveguide Dispersion

In analogy to optical fibers, the dispersion in single-mode dielectric waveguides originates from *material dispersion* and *waveguide dispersion* [9]. *Material dispersion* arises from the frequency-dependent *variation* of the intrinsic material properties (ε_r and μ_r), whereas the *waveguide dispersion* part is due to the frequency-dependent power distribution in the nonhomogenous cross section of the waveguide. Since the intrinsic electromagnetic properties of common low-loss dielectric materials (such as Teflon, HDPE, LDPE) have weak frequency-dependency at mm-waves [9], [10], the contribution of *material dispersion* is negligible. On the contrary, the *waveguide dispersion* affected by waveguide dimensions and geometry as well as the *magnitude* of material properties (ε_r and μ_r) is a strong function of frequency. Fig. 1 shows the obtained generic plots of the normalized phase constant B ($B = [(\beta^2/k_o^2) - 1]/(\varepsilon_r - 1)$, β is the phase constant, and k_0 is the free space phase constant) versus the normalized frequency V ($V = k_o\, r\sqrt{\varepsilon_r - 1} = 2\pi r f\sqrt{\varepsilon_r - 1}/c$, r is the waveguide dimension, and c is the speed of light in vacuum) for the first two modes of common dielectric waveguides made of a low loss HDPE material. The

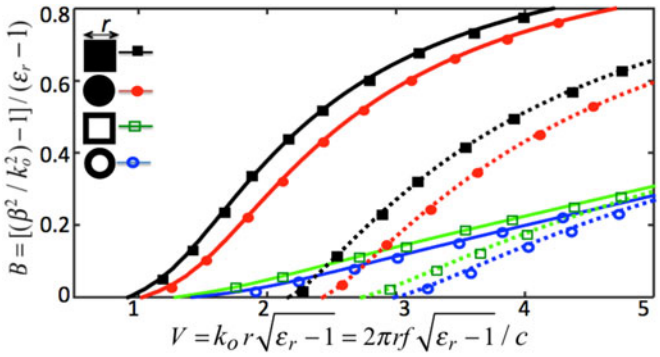

Fig. 1. Simulated results of normalized dispersion B versus normalized frequency V of the first two modes (solid lines: 1st mode, dashed lines: 2nd mode) for different waveguides made of low loss and low dielectric constant HDPE ($\varepsilon_r = 2.25$, $\tan\delta = 0.0003$ [10]). The EM simulation set up is detailed in [11].

single-mode operating bandwidth starts from the $V_{\mathrm{cut-off1}}$ corresponding to the 50% power confinement of the first mode inside the physical waveguide geometry and ends at the $V_{\mathrm{cut-off2}}$ corresponding to the 50% confinement of the higher order mode inside the waveguide. The obtained single-mode bandwidth $\mathrm{BW}_{\mathrm{single-mode}}$ is therefore proportional to the center operating frequency.

The nonconstant B in the operating bandwidth leads to group delay variations. Assuming $g(V) = \beta/k_0$ (defined for simplicity), the group delay per unit length can be calculated as

$$\begin{aligned}\tau_{g,u} &= \frac{\partial\beta}{\partial\omega}\\ &= \frac{\partial(k_0 g(V))}{\partial\omega}\\ &= \frac{\partial k_0}{\partial\omega}g(V)+k_0\frac{\partial g(V)}{\partial V}\frac{\partial V}{\partial\omega}\\ &= \frac{1}{c_0}\left(g(V)+V\frac{\partial g(V)}{\partial V}\right)\end{aligned} \tag{2}$$

which is frequency dependent when g(V) is nonconstant in the operating band. Note that the absolute values of group delay at normalized cut-off frequencies ($V_{\mathrm{cut-off1}}$, $V_{\mathrm{cut-off2}}$, which are fixed for each waveguide) are constant and independent of the center operating frequency.

C. Waveguide Design at 130 GHz

Without loss of generality, the simulated attenuation and group delay of waveguides designed for operating at the center frequency of 130 GHz are compared in Fig. 2(a) and (b). The square and circular rod exhibit the same attenuation and group delay characteristics around the center frequency. Same behavior is observed for hollow circular and hollow square tubes. These similarities are due to similar field distribution on the waveguide cross section [see Fig. 2(c)]. The hollow waveguides exhibit lower attenuation due to smaller portion of the power propagating inside the dielectric [as expected from (1)]. It is interesting to note that in the large portion of single-mode regime [see frequencies $>$ 130 GHz in Fig. 2(b)], the group delay variation of the rod waveguides is less than that of hollow waveguides and approaches to zero. This is because, at these

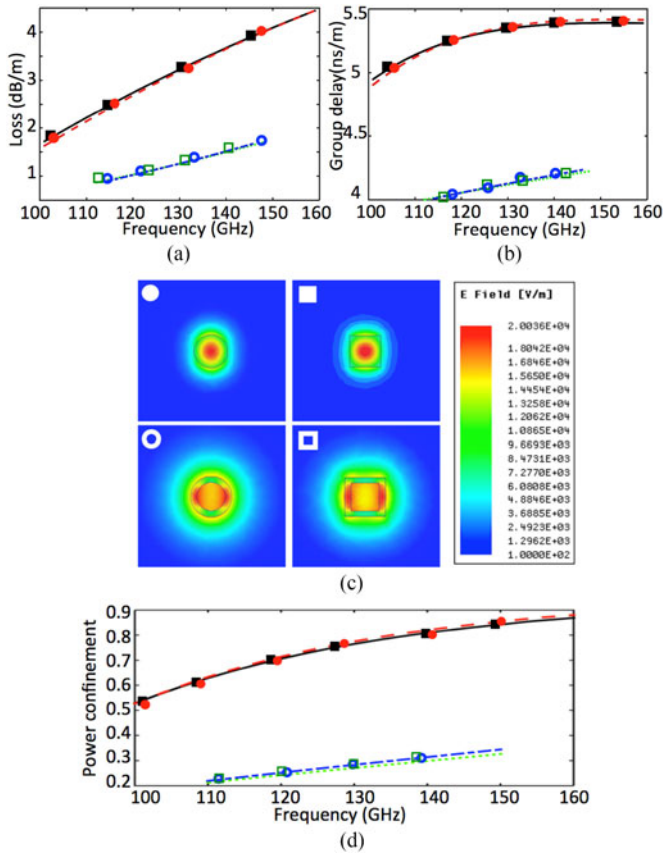

Fig. 2. Full-wave electromagnetic simulation results of (a) attenuation, (b) group delay, (c) electric field distribution at 130 GHz, and (d) amount of energy confined inside the dielectric cross section for different waveguides with the same center operating frequency (waveguide dimension r is 1.5 and 1.58 mm for square and circular rods, respectively, and 1.94 mm for both square and circular tubes (air-to-waveguide ratio is 0.7).

frequencies and for this waveguide, the field is highly confined in the dielectric rod [energy confinement $>$ 80%, see Fig. 2(d)] and the variations of the power confinement and effective permittivity are small. This behavior appears in hollow waveguides at much higher frequencies, where higher order modes already exist [9]. This leads to significantly larger group delay variation in the hollow waveguides in the frequency of interest.

III. Maximum Data Rate and the Corresponding Energy Efficiency

In practice, the required capacity and range determine the choice of waveguide and the operating frequency, which we will show would determine the energy efficiency of the link.

A. Maximum Capacity Limited by Dispersion

In digital data transmission pulse broadening is a limitation on the maximum achievable data rate [12]. In order to avoid intersymbol interference, the interpulse time interval T_{b} which corresponds to the data rate of $\Delta f = 1/T_b$ bit/s, to the first order, must be longer than the broadening time along the link: $T_b > \Delta\tau_{g,\mathrm{link}}$. For example, in OOK or BPSK modulations, the $\Delta\tau_{g,\mathrm{link}}$ is the maximum variations in the band.

In the case of hollow tubes, where the variations of the group delay in the single-mode regime is approximately linear with

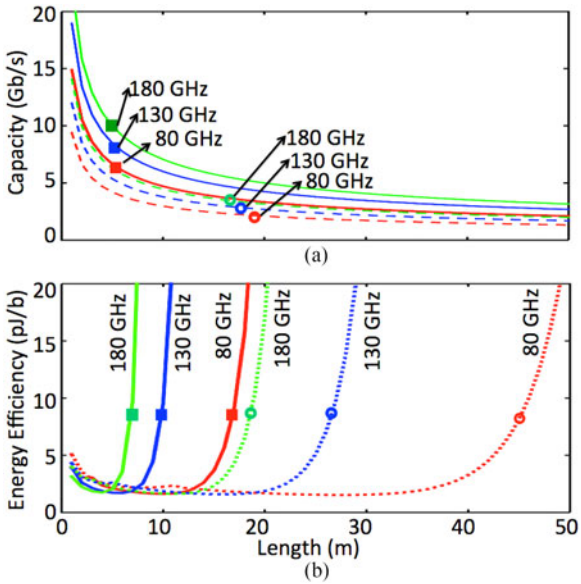

Fig. 3. (a) Maximum applicable bandwidth $\mathrm{BW}_{\mathrm{disp}}$ versus the Length for different waveguides operating at different center frequencies (80, 130, and 180 GHz). (b) The corresponding Energy Efficiency (pJ/bit). Markers represent the type of waveguide cross section.

frequency [see Fig. 2(b)], the maximum achievable data rate for a given distance and operating frequency can be determined as

$$\tau_{g,\mathrm{link}} = \left|\frac{\Delta\tau_{g,u}}{\mathrm{BW}_{\text{single-mode}}}\right| \Delta f l \le T_b = \frac{1}{\Delta f} \tag{3}$$

$$\mathrm{BW}_{\mathrm{disp}} = \Delta f \le \sqrt{\frac{\mathrm{BW}_{\text{single-mode}}}{\Delta\tau_{g,u}\cdot l}} \propto \sqrt{f/l} \tag{4}$$

where $\Delta\tau_{g,\mathrm{u}}/\mathrm{BW}_{\mathrm{single-mode}}$ is the slope of group delay per unit length with respect to frequency. As shown in Section II-B, the maximum group delay variation per unit length in the single-mode regime is independent of the center operating frequency. Moreover, the single-mode bandwidth $\mathrm{BW}_{\mathrm{single-mode}}$ is proportional to the center frequency. Therefore, the maximum applicable bandwidth with tolerable distortion $\mathrm{BW}_{\mathrm{disp}}$ is proportional to $\sqrt{f/l}$. This result is in good agreement with the measurements presented in [5]–[7] and explains the rate limitations. This nonlinear relation of capacity with frequency and the length should be considered in defining new FOMs for such links. Determining the $\mathrm{BW}_{\mathrm{disp}}$ in case of nonlinear group delay (e.g., square or circular rod) is more complicated and is obtained by numerical calculations. Fig. 3(a) shows the maximum applicable bandwidth $\mathrm{BW}_{\mathrm{disp}}$ versus the length for different waveguides operating at different center frequencies (80, 130, and 180 GHz). It shows that the rod waveguide offers a larger $\mathrm{BW}_{\mathrm{disp}}$, which is due to the flat region in the group delay. Moreover, as expected from (4), the $\mathrm{BW}_{\mathrm{disp}}$ increases with increasing the center frequency.

B. Energy Efficiency

As mentioned above, the waveguide and the operating frequency, which are chosen based on the required capacity and range, would determine the energy efficiency of the link. In the transmitter side, to address the link budget, an output power of

$$P_{\mathrm{out,TX}} = -174\,\mathrm{dBm} + 10\log(\mathrm{BW}) + \mathrm{SNR} + \mathrm{NF}_{\mathrm{RX}} + \mathrm{Loss}_{\mathrm{WG}} \tag{5}$$

is required. The BW is $\mathrm{BW}_{\mathrm{disp}}$, SNR is the required SNR at the receiver, $\mathrm{NF}_{\mathrm{RX}}$ is the receiver noise figure, and $\mathrm{Loss}_{\mathrm{WG}}$ denotes the attenuation along the waveguide. We assume a fixed power overhead in integrated circuit modules such as LNA, mixer, and the LO (10 mW each), and conservatively approximate a 5% power efficiency for the power amplifier (PA). We consider a minimum output power of –3 dBm for PA (due to the minimum voltage swing and output impedance). The SNR in (5) is calculated based on BER requirement of 10^{-12} [13], and $\mathrm{NF}_{\mathrm{RX}}$ is assumed to be 10 dB. *Energy efficiency* is thus calculated by dividing the total power consumption to the maximum achievable data rate [see $\mathrm{BW}_{\mathrm{disp}}$ obtained in Fig. 3(a)]. Fig. 3(b) shows the corresponding energy efficiency in terms of pJ/bit. Fig. 3(a) and (b) indicates that for higher data rate we need to operate at higher center frequencies at the expenses of degraded energy efficiency. Moreover, the capacity of such links is not necessarily limited by the attenuation and it can be limited primarily by dispersion.

There is an initial decrease in *energy per bit per length* in the shorter ranges for each operating frequency and waveguide. This is because of the power overhead and as the required $P_{\mathrm{out,TX}}$ exceeds the –3 dBm, the energy per bit per length becomes proportional to the waveguide loss, and exponentially increases with αl (where α is the waveguide attenuation constant and proportional to frequency). There is a *critical length* beyond which the energy efficiency of each waveguide is significantly degraded. At lower frequencies, this critical length is relatively higher at the expenses of lower data rate/pitch [see Fig. 3(a)].

IV. Conclusion

The fundamental physical constraints and tradeoffs in common mm-wave dielectric waveguides are investigated. It is shown that the capacity of such interconnects is primarily limited by the dispersion. Calculations show that the maximum achievable data rate with tolerable distortion are proportional to $\sqrt{f/l}$. Therefore, the link capacity and length determine the choice of waveguide geometry and operating frequency, which determine the energy efficiency of the link. The maximum link length limited by energy efficiency can be extended to larger distances by operating at lower frequencies or using hollow waveguides at the expenses of lower capacity and larger waveguide dimensions. In analogy to electrical or optical interconnects, the capacity of mm-wave dielectric waveguides can be significantly increased by different approaches such as multitone signaling [14], analog/digital equalization [13], waveguide dispersion flattening [12], or using polarization-orthogonal modes of the waveguide [8].

References

[1] E. Wu, "A framework for scaling future backplanes," *IEEE Commun. Mag.*, vol. 50, no. 11, pp. 188–194, Nov. 2012.
[2] C. Hoyeol *et al.*, "Power comparison between high-speed electrical and optical interconnects for interchip communication," *J. Lightw. Technol.* vol. 22, no. 9, pp. 2021–2033, 2004.

[3] C. Kachris *et al.*, "A survey on optical interconnects for data centers," *IEEE Commun. Surveys Tuts.*, vol. 14, no. 4, pp. 1021–1036, Oct./Dec. 2012.
[4] A. V. Krishnamoorthy *et al.*, "Progress in low-power switched optical interconnects," *IEEE J. Sel. Topics Quantum Electron.*, vol. 17, no. 2, pp. 357–376, Mar./Apr. 2011.
[5] S. Fukuda *et al.*, "A 12.5+12.5 Gb/s full-duplex plastic waveguide interconnect," *IEEE J. Solid-State Circuits*, vol. 46, no. 12, pp. 3113–3125, Dec. 2011.
[6] Y. Kim *et al.*, "High-speed mm-wave data-link based on hollow plastic cable and CMOS transceiver," *IEEE Microw. Wireless Compon. Lett.*, vol. 23, no. 12, pp. 674–676, Dec. 2013.
[7] W. Volkaerts *et al.*, "An FSK plastic waveguide communication link in 40nm CMOS," in *Proc. IEEE Int. Conf. Solid-State Circuits*, 2015, pp. 1–3.
[8] N. Dolatsha *et al.*, "Fully-packaged mm-wave dielectric waveguide with multimode excitation," *Electron. Lett.*, vol. 51, no. 17, pp. 1339–1341, 2015.
[9] C. Yeh *et al.*, *The Essence of Dielectric Waveguides*. New York, NY, USA: Springer, 2008.
[10] M. Afsar *et al.*, "Precision millimeter-wave measurements of complex refractive index, complex dielectric permittivity, and loss tangent of common polymers," *IEEE Trans. Instrum. Meas.*, vol. 1001, no. 2, pp. 530–536, Jun. 1987.
[11] A. Patrovsky *et al.*, "Substrate integrated image guide (SIIG)-a planar dielectric waveguide technology for millimeter-wave applications," *IEEE Trans. Microw. Theory Techn.*, vol. 54, no. 6, pp. 2872–2879, Jun. 2006.
[12] S. J. Orfanidis, "Group velocity dispersion and pulse spreading," in *Proc. Int. Conf. Electromag. Waves Antennas*, 2014, pp. 99–103.
[13] H. Nguyen *et al.*, *A First Course in Digital Communications*. Cambridge, U.K.: Cambridge Univ. Press, 2009.
[14] A. Amirkhany *et al.*, "Multi-tone signaling for high-speed backplane electrical links," in *Proc. Int. Conf. Global Telecommun.*, 2004, pp. 20161111–1117.